Renewable Energy 115 (2018) 1055–1066

Contents lists available at ScienceDirect

Renewable Energy

journal homepage: www.elsevier.com/locate/renene

Wave resource characterization through in-situ measurement followed by artificial neural networks' modeling

Antonio Santos Sánchez [a, *], Diego Arruda Rodrigues [a], Raony Maia Fontes [a], Márcio Fernandes Martins [a], Ricardo de Araújo Kalid [b], Ednildo Andrade Torres [a]

[a] Federal University of Bahia, Brazil
[b] Federal University of South Bahia, Brazil

ARTICLE INFO

Article history:
Received 18 November 2016
Received in revised form
7 September 2017
Accepted 9 September 2017
Available online 13 September 2017

Keywords:
Wave energy
Wave monitoring
Artificial neural network
Resource assessment

ABSTRACT

This research presents a mathematical model that uses artificial neural networks for the assessment of the wave energy potential of sites, based on data recorded by wave monitoring instrumentation. The model was implemented and validated in two different sites. The first one had a dataset from an upward-looking acoustic Doppler current profiler that recorded a hindcast during 2½ years. The second consisted in data from a buoy using motion sensors that recorded continuously during 23 years. For this second site, the performance of the neural network model was compared to that of the Nearshore Wave Prediction System (NWPS), which combines SWAN, Wavewatch III and other numerical models. For the 2½ years' hindcast, the error of the neural network was significant which suggests a better use for filling missing gaps within datasets than for resource assessment. Meanwhile the performance of the neural network trained with the 23 years' hindcast was satisfactory; better than the NWPS in terms of relative bias but worse in terms of scatter index. Therefore it is concluded that neural networks can make an optimal use of the data produced by wave monitoring instrumentation and are useful to characterize the wave energy resource of a coastal site.

1. Introduction

1.1. Justification and objectives

Waves are a promising energy resource, although intermittent and unpredictable. The use of this renewable source has two front lines. The first one is the development of more efficient and economical electromechanical conversion devices. The other one is the development of methods to assess precisely the energy potential of sites in which wave power plants could be located. At present, wave energy is only economically viable if subsidized, due to its higher levelised costs when compared to other energy sources [1]. In parallel with development of wave converter prototypes, deployment strategies that aim to reduce costs include the installation of wave energy devices in existing marine structures, such as breakwaters, and the combination of offshore wind and wave energy arrays.

Certainly, waves are a renewable energy source that raises an increasing interest. Year after year new researches are published regarding local wave potential assessments around the world; some recent examples can be found in Refs. [2-6]. Most of this research is based on the application of third-generation wind-wave models, sometimes improved with different mathematical models that consider complementary aspects such as, for instance, the directional spectra transformation from open ocean to the nearshore. Third-generation wind-wave models provide wave spectra and wave field information over large selected sea areas. The models are particularized to a geographical area by considering its bathymetry and local currents. Then the wave forecasting model makes predictions with some days in advance based on wind speed at sea. If a record of average wind speed data is used as input, the model can generate a hindcast from which the local wave energy potential can be inferred. These available computational models are primarily intended for climate monitoring and navigation, but have interesting applications for the assessment of wave energy potential.

Some wind-wave models are able to accurately reproduce the wave climate and, therefore, the energy available, in very shallow

* Corresponding author.
E-mail address: sanchezbahia@gmail.com (A.S. Sánchez).

http://dx.doi.org/10.1016/j.renene.2017.09.032
0960-1481/

waters. The model can be further tuned by using data assimilation, a process in which real wave measurements are incorporated into the model state of the numerical model. This results in very accurate models that go beyond preliminary evaluations of energy resource. Through the use of these numerical models, large areas can be assessed and the sites with the greatest potential can be revealed.

A different approach is considered in this work, as our proposal refers to the use of wave data measured in a particular site, followed by further statistical processing of those data. The aim is to perform a detailed evaluation of the energy that a site would produce and therefore an analysis of the profitability of a wave energy plant located in that site.

Our proposal intends a methodology that is simpler than conventional numerical models and shows two advantages over them: (I) requires much less computing power; and (II) is capable of using incomplete hindcasts, estimating the values of the gaps between measurements with an acceptable error. Regarding this second issue, it must be mentioned that simulations using numerical modeled data have been used for energy predictions, however they cannot substitute numerical modeling techniques, particularly if there is not enough buoy or recording data [7-10]. International protocols and resource assessment methods require at least 10 years of dataset, in order to ensure that the seasonal, intra-annual and decadal variations are resolved [11-13]. The proposed method could be very useful especially for sites with less than 10 years of continuous dataset. That's why a 2½ years hincast is used for developing and testing this proposal, using real data for validation and estimating the error. Further on, the model will also be tested using a much comprehensive hindcast (23 years) in order to compare it with a state-of-the-art nearshore numerical model.

The starting point of this method is in-situ data acquisition using field instrumentation, such as ondographs or wave profilers, generating a record of direct measures.

The recorded data is then used as input for a computational algorithm based on an artificial neural network (ANN) that develops a wave energy model for the site. Independently from the length of the hindcast of the site, the model can generate wave data for extended periods of time, enough to characterize the wave energy potential of the site with a reasonable error. It is this feature where the strength of the model lies: a small, incomplete set of wave data is enough to generate an approximation of the wave resource behavior in the site. Certainly, the accuracy of this approximation would depend on the length of the wave database, and so one of the objectives of this work would be to validate the model using real wave data and assess the resulting error.

It is noticeable that artificial neural networks (ANNs) have been used during past years to develop wave forecasting models or to improve incomplete wave parameters hindcasts, as shown in Table 1:

The type of ANN most commonly found in the reviewed literature coincides with the one proposed in this work: a three-layer feed-forward networks with a non-linear differentiable log–sigmoid transfer function in the hidden layer and a linear transfer function in the output layer.

Two main categories are found among the reviewed scientific literature. The first category represents temporally univariate models, in which current and previous wave data are used to forecast future wave data from a few hours to a few days in advance. The ANN model proposed in this work lies within this one. The second category represents cause-effect models in which the cause (wind data) has been used to forecast wave date.

The originality of this research with regards to previous literature consists in the application of ANN models to the assessment of the wave energy of a site and also, in the use of wave measurements obtained through field instrumentation as input for the model. Particularly, it was used an upward-looking acoustic Doppler current profiler. The use of direct wave measures instead of wind or other related data is emphasized in this method, and so a review of field instrumentation for wave measurement is presented on the next chapter. In addition, for the first time in South America, a hindcast of real wave data is used to assess the potential of this renewable energy source in a site. The developed model could be used for further assess the wave energy potential in all the network of wave measurement stations recently deployed in Brazil (see chapter 1.3) as well as in similar wave monitoring sites worldwide.

Moreover, we hope that this work highlights the contribution of artificial intelligence, in the form of self-learning algorithms, to the assessment of the waves' energy potential.

1.2. State-of-the-art of wave measurement

The measurement of the wave climate plays a vital role in the identification and monitoring of potential sites for commercial developments of marine renewable energy (MRE). Wave measurement is also needed in the development of MRE converters, during testing phases at model scale in a controlled environment up to testing phases at full scale out at sea [34]. Nowadays, a broad set of technologies are available for the measurement of ocean wave fields under different conditions, either controlled wave tanks or open sea conditions. They are also valid for a wide range of scales, from the detailed assessment of the wave energy potential of a particular site to the monitoring of extent ocean areas.

Remote sensed satellite measurement, or the use of altimeter radars placed in satellites, is widely used for the measurement of ocean's bathymetry and topography as well as for wave measurements. Altimeter radars measure the height of the satellite above the sea surface. When applied to wave measurement, the radar emits radio pulses that reflect first from the wave crests and later from the wave troughs. The time delay of the reflection pulse is used to calculate the wave height. Although the resolution and accuracy are poorer than in-situ measurement, they have the advantage of covering wide areas and therefore are used primarily for the validation of global ocean models. In addition, a fleet of commercial ships (Voluntary Observing Ships) equipped with different types of on-board instrumentation provide ground validation of remote sensed satellite measurement.

Satellites launched during the last decades such as Topex/Poseidon (1992–2001), Jason1 (2001) and Jason2 (2008) were specially designed to make extremely accurate measurements of sea-surface height: accuracy is ±0.05 m [34]. Therefore, radar altimeter data have allowed the real-time monitoring of wave-heights, initiating a new era of wave climate measurement. Nowadays these data are used worldwide for navigational, scientific and even recreational uses (surf). When applied to the characterization of wave energy resource, radar altimeter data allow the study of the variability of wave energy density in time and space.

Beyond height measurement, the emphasis is put nowadays on measuring the directional spectra of ocean waves [34]. Information about the directional behavior of wave fields complements the energy resource assessment of a site. Together with height and period, direction is the most important parameter to be studied in order to characterize the energy potential of a site. Arrays of remote-sensing instruments, such as laser altimeters or ultrasonic transducers, return point-measurements and can be used to measure the directional properties of ocean waves propagating over smaller areas. Stereo-photogrammetry is another technique that can provide information about the directional characteristics of the wave field in a small area. Currently, space-borne synthetic aperture radar (SAR) is the only instrument providing directional ocean

Table 1
Literature review of wave models using artificial neural networks.

Type of ANN (artificial neural network) model	Location of the study	Year	Ref.
Three-layered feed-forward, trained through L-M optimization; hyperbolic tangent sigmoid and linear transfer functions	NE Brazil	2017	This research
MIKE21 SW (Spectral Waves) model coupled with an ANN of 3 layers; L-M optimization; sigmoid and linear transfer functions	India	2016	[14]
Three-layered feed-forward, trained using a multilevel neuro-wavelet transform	Gulf of Mexico (USA)	2015	[15]
Three-layered feed-forward ANN combined with wavelet fuzzy logic, fuzzy logic and autoregressive moving average	Pacific Coast (USA)	2010	[16]
Three-layered feed-forward, with conjugate gradient, L-M optimization, resilient back propagation and quick propagation	India	2007	[17]
Three-layered feed-forward, trained with standard backpropagation (Rprop algorithm)	India	2006	[18]
Three-layered feed-forward optimized with a CFC conjugate gradient algorithm	Gulfs of Alaska, Mexico and Maine (USA)	2006	[19]
Different ANNs simulating wave parameters and working in parallel	Portugal	2006	[20]
		2005	[21]
Three-layered feed-forward, trained with supervised back propagation	Tasmania (AUS)	2007	[22]
		2005	[23]
	NW Pacific Ocean	2006	[24]
	India	2005	[25]
		2001	[26]
		1998	[27]
		1997	[28]
	Ireland	2004	[29]
	Taiwan	2001	[30]
Static feed-forward multilayer neural networks coupled with the stochastic auto regressive and exogenous input auto regressive models	Turkey	2004	[31]
Three-layered feed-forward, trained with back propagation, conjugate gradient and cascade correlation	India	2002	[32]
		2000	[33]

wave information on a global scale. New space-borne missions using interferometric SAR technology for the measurement of ocean waves and currents have already been planning for the next years [35].

Remote measurement is essential for the monitoring of the weather and climatic conditions of wide areas as well as for the validation of numerical models. It can also provide primary data for the selection of sites with significant wave energy potential. Once focused in a particular area, in-situ measurement provides a detailed characterization of the local wave conditions. The uncertainty of the in-situ measurement can be minimized with a correct selection of the measuring technique and the instrument positioning, as well as with the initial verification of instrument accuracy followed by periodical calibration and maintenance.

Capacity sensors, pressure-velocity sensors and buoys are the most basic instrumentation available for in-situ measurement of ocean gravity waves. Those mature techniques have been used for decades. Pitch-and-roll buoys are widely used but they are expensive, prone to damage and vandalism, and have mooring issues in shallow coastal waters [34]. Other option is the installation of arrays of capacitance wire gauges or bottom-mounted sensors. Among the latter, pressure-velocity (PUV) sensors are less expensive but are limited in effective working depths to less than 10–15 m due to the high degree of attenuation in the high frequency portion of the wave signal of pressure and velocity [34].

The above-related methods have been complemented with a set of new technologies, subsequently reducing the uncertainty of the wave measures. The first type of new technologies that have come to complement the traditional ones are radars, particularly marine X-band radars, coastal High Frequency (HF) radars and real or synthetic aperture radars. Nautical radars allow scanning the sea surface with high temporal and spatial resolution. They can be mounted on ships, buoys or coastal stations and allow taking site-wide sea state measurements from the backscatter of microwaves from the rough sea surface. Other new types of instruments are Acoustic Doppler Current Profilers (ADCPs), lidars (laser-based instruments), displacement and GPS buoys and, more recently, stereo vision methods that have allowed the measurement of three-dimensional wave fields.

The spatial and temporal scales required for the study of water wave dynamics are different out at sea from those needed at model scale (in a wave tank laboratory). For instance, resistance-type gauges are commonly used for wave measurement in hydrodynamics laboratories. They are reliable and robust, but if deployed at sea large measurement errors can occur due to water currents moving the gauge device. Other instrumentation generally used in laboratories are capacitance wave gauges (less intrusive than resistance-type gauges), mechanical profile followers or pressure sensors combined with velocity sensors.

Non-intrusive instrumentation is preferable against in-situ instruments, as the first one does not interfere with the wave field to be measured which is an advantage in laboratory experiments as it reduces disturbances. The wave field can be disturbed due to radiated waves generated at the intrusive instrumentation (probe), which becomes more important as the scale of the waves considered decreases.

In addition, when deployed at sea, non-intrusive instrumentation suffers less exposure to sea water corrosion, bio-fouling, wave load and damages from human activities, and therefore requires less maintenance.

Fig. 1 summarizes these non-intrusive techniques available for wave measurement.

This research is based on data acquired with an Acoustic Doppler Current Profilers (ADCP) deployed on the seabed near the shore. ADCPs are non-intrusive and have been successfully adapted to the measurement of directional wave spectra. They measure the water velocities over a depth range using the Doppler effect of sound waves that are scattered back to the acoustic beams of the instrument. ADCPs use generally at least three acoustic beams so they are able to estimate the directional properties of the wave field. The particular ADCP used in this research, namely Teledyne RDI Workhorse wave array, allowed measuring the multi-

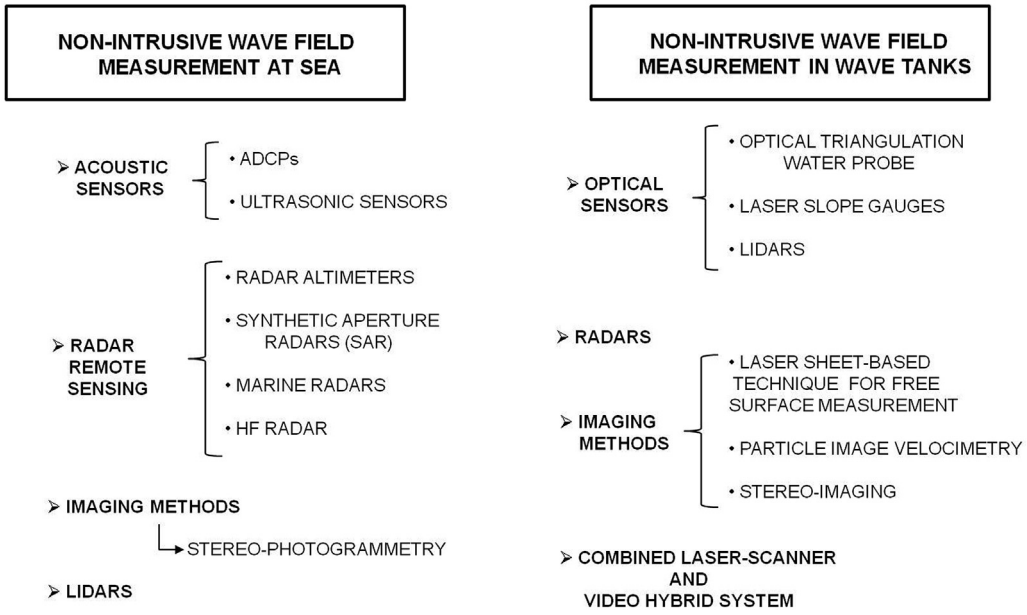

Fig. 1. Scheme of non-intrusive techniques for wave measurement.

directional wave spectra, current velocity profiles, and water level at the same time. This was possible by using up to a total of 12 radial velocity measurements to quantify the near-surface orbital fluctuations at up to three different depth levels as inputs for the directional spectra measurement [36].

ADCPS can be installed under the sea level or at the surface. Some researches have compared a surface tracking ADCP (AWAC from Nortek) and a submarine ADCP (RDI workhorse wave array), concluding that the surface tracking is more precise but is also susceptible to false returns from bubble clouds generated by extreme wind-wave conditions or by boat wakes and wash [37,38]. Seim and Edwards (2006) also did a comparative study between a buoy-mounted ADCP and a bottom-mounted, upward-looking ADCP detecting some noise and interference problems inherent to the buoy-mounted ADCP, which are avoided when using submarine ADCP [39].

1.3. Brazil's wave monitoring programs

The lack of enough experimental data is a conditioning factor for the modeling of the wave's behavior in the Brazilian coast. That turns necessary the use of mathematical simulation models that take as inputs other secondary climatic data, for instance the wind speed at the sea level. The CPTEC - Brazilian Center for Weather Forecasting and Climatic Research uses the third-generation model for oceanic waves WAVEWATCH 2.22, which is suitable for waters with more than 40 m' depth. This model is directed for marine navigation, not for assessing the energy potential of waves on the shoreline. Nevertheless, the WAVEWATCH III (WW3) model has already been used to assess the wave potential in parts of the Brazilian seashore [40]. Among the few researches using experimental data are Beserra et al. (2007) [41] who used a 5-year pitch-roll buoy data series to assess the energy resource in the North coast of the country and Assis (2010) [42] who investigated the Southern coast of Brazil using a 2.5-year pitch-roll buoy data series.

One of the most remarkable initiatives for establishing a wave monitoring network around the country's shore is the PNBOIA - Brazilian National Buoy Program. It consists in a network of drifting buoys and fixed buoys anchored in the shoreline that are tracked by satellite, with the aim to provide real-time weather and oceanographic data. This program has propitiated both the gathering of scientific knowledge and a contribution to weather and oceanographic forecasts.

The most recent Brazilian wave monitoring network, starting in 2013, is called “Rede Ondas”. This network counts with ondographs and wave profilers located on the seabed under shallow waters in eight sites of the country's shoreline (see Fig. 2). This network is coordinated by the Brazilian Navy and supervised by GOOS - The Global Ocean Observing System, an international cooperation platform from which Brazil is member. This network is expected to complement the PNBOIA buoy system and to provide more detailed information about coastal erosion and the impacts of climatic change. For the first time data from the “Rede Ondas” system are also used to estimate electricity generation potential. In this research, data recorded at intervals of 3 h during 30 consecutive months in one of the “Rede Ondas” stations were used to develop a mathematical model of the energy potential in the site where the station is located.

2. Methodology

2.1. Data gathering

Wave data were recorded with an Acoustic Doppler Current Profilers (ADCP) Work Horse Sentinel that operates at a frequency of 600 kHz and is equipped with a directional wave meter - *Waves Array* from Teledyne RD Instruments. This device operates in Praia de Forte (State of Bahia) at latitude 12° 36′ 13.8″ South and longitude 37° 58′ 31.8″ West. It is deployed on the seabed under the 32 m' isobath, fixed to an anti-drag concrete structure. Fig. 3 shows the operation of this metering device.

This instrument measures the significative wave height, the wave peak period and the direction of the waves. In other words, it measures the complete frequency/direction wave spectrum. Measures are taken at intervals of 3 h within a “burst sampling” mode at a frequency of 2 Hz. Although this device allows transmitting the measures to shore via a cable link or acoustic modem as real-time data, in the “Rede Ondas” network data are stored internally for

Fig. 2. The "Rede Ondas" Brazilian wave monitoring network, based on anchored ondographs and seabed-deployed wave profilers.

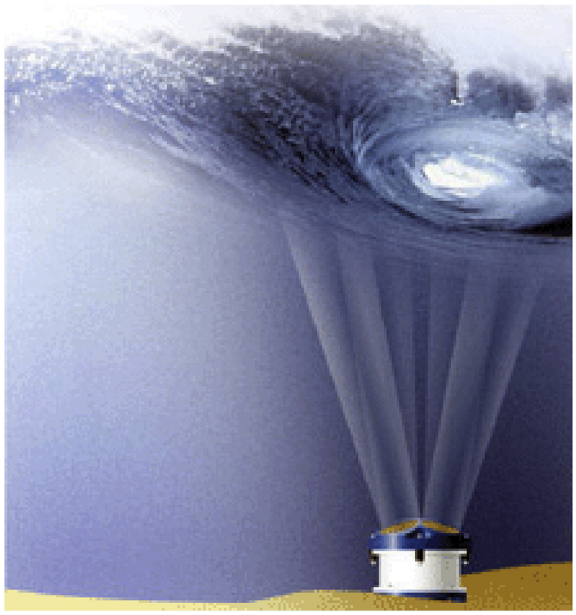

Fig. 3. Scheme of the Acoustic Doppler Current Profiler used for data acquisition [43].

short or long-term deployments. Divers recover the stored data every month.

The uncertainty of the ADCP's primary sensors under the field conditions in which it operates is excellent [43]. Regarding tilt, both accuracy and precision are ±0.5° with a resolution of 0.01°. Regarding the fluxgate-type compass, it includes a built-in field calibration feature that allows an accuracy of ±2°[5] and a precision of ±0.5°[5] with a resolution of 0.01°. The profile parameters are velocity (accuracy ±0.3 cm s^{-1}, precision ±0.1 cm s^{-1}) and echo intensity profile. The latter has a precision of ±1.5 dB which gives a velocity resolution of 0.1 cm s^{-1}. Using those primary measures, the ADCP internal software calculates height, period and direction. Then, after the burst sampling, the mean values of height and period are calculated and stored in the internal memory as the representative values of that 3 h' period.

It is worth noting that the ADCP records the wave peak period, which corresponds to the wave period with the highest energy. In order to estimate the power of wavefronts in the site, the wave peak period must be converted to wave energy period, which is the mean wave period with respect to the spectral distribution of energy. The conversion to wave energy period was done considering the waves characteristics as within the JONSWAP spectrum [44], from which the Bretschneider (one-sided) ocean wave spectrum is the limiting form [45]. In that case, some authors suggest a wave energy period/peak period ratio of 0.85 [46]. This study adopted a value of 0.9 which is equivalent to assuming a standard JONSWAP spectrum with a peak enhancement factor of 3.3 [45].

2.2. Power estimation of wavefronts

In Physics, a wave is defined as an energy transport phenomenon that transports energy along a medium without transporting matter. The amount of energy carried by a wave is directly proportional to the square of the amplitude of the wave. An ocean wavefront can be defined as an advancing surface of wave propagation, and follows that behavior. The amplitude corresponds to the height of the wavefront, a parameter that is measured by the wave profiler. The height would determine the maximum of kinetic energy that is carried within each wave. In addition, by considering the period between consecutive wavefronts, it can be calculated the potential power (energy per unit time) that could be generated given a specific sea conditions (wave's period and height). A wave energy device located under those conditions would harvest only a percentage of that maximum theoretical potential. The water density (ρ) also influences the power that can be extracted from a wave: denser, saltier waters carry more kinetic energy than softer waters at similar conditions.

Calisal (1983) calculated the energy density of a developed two-dimensional wave, giving the total energy expressions for deep and finite depth water waves [47]. In deep water waves the potential energy density propagates with the phase velocity, while the kinetic energy density is stationary. For surface waves propagating at a finite depth the kinetic energy density has a stationary and a propagating component, and the portion of energy travelling with the phase speed is the potential energy. The power resource from a wavefront is determined by the water density (ρ), gravitational acceleration (g) and the wave's amplitude (A) [47]:

$$P = \frac{1}{2}\cdot\rho\cdot g\cdot A^2 \tag{1}$$

This expression can be simplified to obtain another one that only depends on the wave's height (H) and the period between two consecutive wavefronts, that is, the wave energy period (T) [48]:

$$P = \frac{\rho\cdot g}{64\cdot\pi}\cdot H^2\cdot T \approx \frac{1}{2}\cdot H^2\cdot T \tag{2}$$

The above expression, Eq. 2, calculates the power per meter of wavefront (kW m^{-1}) for the height H in meters and the wave energy period T in seconds. Eq (2) is only valid for deep waters where the waves do not interact with the bottom and wave characteristics are thus independent of the water depth. To fall within this category, data must complain with the criteria d/L > 0.5 (d = depth, L = wave length). That is the case of this study as the ADCP was deployed under the 32 m isobath. For wave power potential at shallow waters, Eq. 3 is more appropriate:

$$P = \frac{\rho\cdot g}{32\cdot\pi}\cdot H^2\cdot T \tag{3}$$

An alternative method of power calculation is described by Pitt (2005) [49]. That method also calculates the power were the wave system is unidirectional, regardless the wave spectral direction. However, the significant wave heights are calculated from the spectral wave characteristics. The wave spectra is measured over different frequency ranges with different frequency subdivisions. The power per meter of wavefront is calculated using Eq. 4:

$$P = \rho\cdot g\cdot \sum_{i=1}^{i=64} S_i\cdot V_g(f_i)\cdot \Delta f_i \tag{4}$$

where $V_g(f_i)$ is the velocity at the i^{th} frequency, S_i is the corresponding spectral density estimate, Δf_i is the i^{th} frequency subdivision, ρ is the density of seawater (1025 kg m^{-3}) and g is the acceleration due to gravity (9.8184 m s^{-2}).

Eq. 4 is less intuitive, although may be adequate for some wave measurement techniques, such as radar/Waverider buoys [34]. As the database used in this research consists of records of height and period, it was considered Eq. 2 as the most suitable expression for the wave power estimation.

2.3. Development of the neural network model

Artificial neural networks (ANN) can be described as machine learning models that mimic a human neural system. An artificial neural network is a structure of information processing that approximates functions that can depend on a large number of unknown inputs. Their ability to be used as an arbitrary function approximation mechanism that 'learns' from observed data is an important advantage. That is, they can be used to infer a function from observations.

ANN models are trained using historical data record that represents the behavior of a system. Once trained and optimized, such model takes as inputs the data from the previous instants (the previous values of one or more variables). The model processes the inputs and gives, as output, the forecasted values for a selected set of variables according to the historical behavior of the system. Between the input and the output, there may be one or more hidden layers, each consisting of a number of processing units called neurons that together form a self-learning algorithm.

Generally, the number of input variables would determine the complexity of the model. These input neurons send data to following layers of neurons, but during this process some parameters are stored. Those stored parameters are called the “weights” of the interconnections and manipulate the data in the calculations. The “activation function” converts a neuron's weighted input into its output. The output is then compared and the weights are adjusted (updated) through a learning process, using a “cost function”. This function is a measure of how far away a particular solution is from an optimal solution. Therefore, in the validation (comparison) period an error index must be adopted for measuring the success of the forecasting.

The model structure may be a simple feed-forward. However, the power output generated at any hour may present some correlation with the one from the previous hour. This would be the case of weather events, such as storms or anticyclones, lasting even several days. During those events the waves' height and period would be particularly high or low. The accuracy of the forecasting model can be improved by using a more evolved structure that considers possible correlations between the previous outputs (the wave power from previous hours) and thus detects those eventual climatic events, adjusting the prediction. For that reason it was chosen a non-linear autoregressive exogenous model (NARX). Such structure consists basically in the feedback of the ANN using outputs from previous moments as feed-forward inputs. This approach is commonly used as a way to represent dynamic systems [50–53]. Thereby, the model uses values from past variables to make future predictions, as in a dynamic system model like the one presented in Eq. 5:

$$y(t) = f\left(y(t-1), y(t-2), \ldots, y\left(t-n_{ty}\right), u(t-1), u(t-2), u(-n_{tu})\right) \tag{5}$$

The final structure of the ANN is represented in Fig. 4:

Having defined the model's structure the next step is to define the final architecture. That is, the type of the activation function of each neuron, the number of hidden layers and the number of their neurons and finally the selection of the best model. It was already demonstrated that one single layer is enough for a neural model to

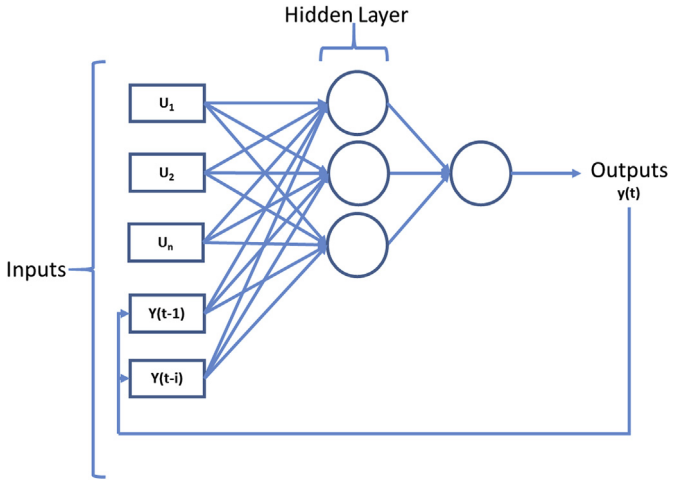

Fig. 4. Structure of the chosen neural network model: non-linear autoregressive exogenous model.

be able to approximate any function with an arbitrary precision [54]. The activation functions must be chosen according to the system that is under study such, for example, in the case of pattern recognition in which step functions are commonly used. Regarding the training stage, the most common method used is back-propagation [55–58]. This method consists in the continuous adjustment of the network parameters until its prediction is as close as possible to the experimental data. After the selection of the activation functions and the training methods, we arrive to the crucial point of the model, which is choosing the number of neurons in the hidden layer. This number will determine the quantity of parameters to be estimated during the training stage. Too many neurons may lead to overadjustment, that is, the unwanted modeling of noise or spurious data. Meanwhile, a less-than-necessary number can have a detrimental effect on the quality of the model's prediction. In 1996, Schenker and Agarwal [59] proposed the use of dynamic cross-validation for the selection of the optimal number of neurons of the hidden layer, demonstrating the efficiency of this methodology when applied to cases with little available data. In the present work, the number of neurons was used through dynamic cross-validation. The method consists in separating the data in three groups, namely A, B and C. Groups A and B will be used for training two different networks for each neuron number. After the training, the network developed using data group A is validated with data group B. The model predicts the values of data group B and the resulting error is calculated. The process is repeated, increasing each time the number of neurons until reaching a maximum of 40 neurons. The number of neurons that shows the lowest validation error will be taken as the optimum. This error, calculated as the minimum mean square error, is represented versus the number of neurons in Fig. 5. It can be observed from the figure that the lowest validation error corresponds to a hidden layer of 2 neurons.

After the selection of the number of neurons of the hidden layer, the final step is the training and validation of the final structure. The training consists in estimating the parameters of the neural network: weights and bias. Those parameters are estimated through a problem of optimization. To solve that problem, it was used the Levenberg-Marquardt backpropagation algorithm. In order to avoid the overadjustment of the data by the model, the early stopping technique was used. The overadjustment problem arises when the network is overloaded with information about the training group and has its capacity degraded [59–61]. The early stopping technique consists in stopping the training after a successive number of iterations, when it is noticed that the validation error increases. The training of the final network was done with data groups A and B, while the validation was done with data group C. Approximately 10% of the data were used to predict the remaining 90%. The general definitions of the final model are shown in Table 2.

2.4. Measuring the model prediction error

The accuracy of the load prediction of a neural network or any other mathematical model is usually defined using two terms: the Mean Absolute Percentage Error (MAPE) and the coefficient of variation (CV).

The MAPE, also known as mean absolute percentage deviation, is usually expressed as a percentage and is widely used for measuring the accuracy of a forecasting method or trend estimate. It is very intuitive as refers to the innate concept of the error as the difference between the real and the forecasted values. It is defined by the formula:

$$MAPE = \frac{1}{n} \cdot \sum_{t=1}^{n} \left| \frac{P_t - F_t}{P_t} \right| \cdot 100\ (\%) \tag{6}$$

where P_t is the actual value (the measured power in the instant t) and F_t is the forecast value for that instant. The difference between P_t and F_t is divided by the actual value P_t again and the absolute value of the resulting division is summed for every forecasted point and divided by the number of fitted points n.

In this research the ANN model is used to forecast the potential power that could be harvested from the waves during 10 consecutive months (at a rate of one prediction each 3 h). In order to assess the precision of the model, the error of each predicted value is calculated by particularizing the MAPE expression for each one of the forecasted points:

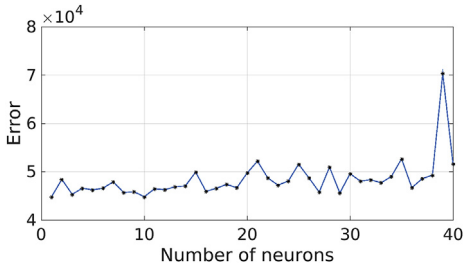

Fig. 5. Dynamic cross-validation for the selection of the optimal number of neurons of the hidden layer: validation errors for different number of neurons.

Table 2
Characteristics of the proposed ANN model.

	ANN model parameters
Total number of neurons evaluated	40
Total number of trainees done	15
Optimal number of neurons	2
Total iteration in training step	1000
Performance (mse)	7.02
Minimum gradient	10^{-7}
Early stopping criteria	30
Transfer function in the first layer	Hyperbolic tangent sigmoid
Transfer function in the output layer	Linear function

$$Error = \left|\frac{P_t - F_t}{P_t}\right| \cdot 100(\%) \quad (7)$$

Both the predicted and the measured values during the 10 months' timeframe are displayed together in the following chapter, as a "validation" of the model. This error corresponds to the accuracy of the model, or the proximity of predicted results to the true value.

The errors of all the forecasted points are also classified within a histogram in order to assess their frequency distribution. We chose to do this as gives an insight of how distributed the errors are, complementing very well the information provided by the MAPE. This option is more graphic and didactic than the calculation of the coefficient of variation (CV). That coefficient, also known as relative standard deviation, is a standardized measure of dispersion of a probability (frequency) distribution, defined as the ratio of the standard deviation to the mean or to the absolute value of the mean:

$$CV = \frac{\sigma}{\mu} \cdot 100(\%) \quad (8)$$

where σ is the standard deviation and μ is the mean. While the MAPE is related to the accuracy of the model, an assessment of the error distribution either graphically or through the use of the CV, is related to the concept of the precision of the model expressed as the closeness of agreement among its set of results.

3. Results and discussion

3.1. Model output, performance and error distribution

It was used a database consisting of 6312 measures of height and period, which originated the corresponding power values. The experimental data correspond to a recorded power between 1 and 65 kW m^{-1}. The total incoming energy during the 30 months was 179 MWh per meter of wavefront.

A fraction of the data set was applied in the developing of the model. Specifically, 3156 values were used to train the neural network. Later, the model was used to predict the power in all the points (validation of the model). The result of that validation is shown in Fig. 6:

The error distribution, shown in Fig. 7, revealed a slight trend of the model to overestimate the power. The mean value of all the errors was +7.2%.

The resulting set of errors showed a distribution with a small standard deviation. The standard deviation indicates how close the data points tend to be to the mean of the set of errors. For the set of errors produced by this model, the standard deviation (sigma) is

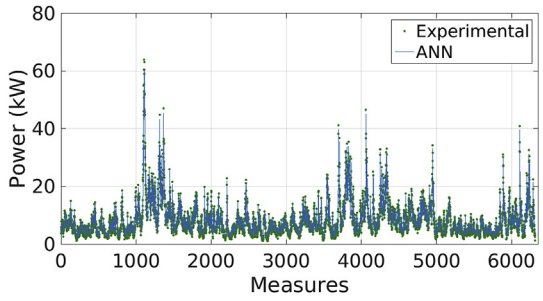

Fig. 6. Validation of the model: experimental data (green points) VS ANN model (blue line). (For interpretation of the references to colour in this figure legend, the reader is referred to the web version of this article.)

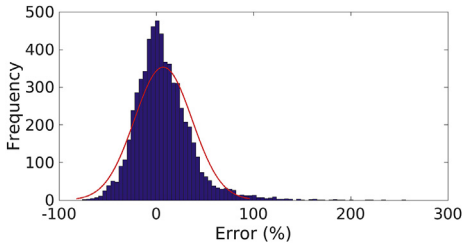

Fig. 7. Distribution of the errors made by the model.

29.60%. However, the model made some gross errors of up to −70% and +260% at some points.

Together with the histogram of errors, Fig. 7 depicts the normal (or Gaussian) distribution of errors. This function is symmetric around the point +7.2 (mean value of the error). Within a normal distribution, the 3-sigma rule establishes that 68% of values are within one standard deviation away from the mean; about 95% of the values lie within two standard deviations; and about 99.7% are within three standard deviations.

Therefore it can be stated that by using the proposed ANN model, 68% of the forecasted values have an error of between −22.4% and +36.8% (MAPE ≤ 29.8%); 95% of the forecasted values have an error of between −52.0% and +66.4% (MAPE ≤ 59.2%); and about 99.7% of the forecasted values have an error of between −81.6% and +96.0% (MAPE ≤ 88.8%).

The validation of the proposed ANN model using a 2½ years' dataset showed an average error in the estimate of 7.2%, which is above the error of properly set up models that use extent hindcasts [62-65]. That error together with the high deviation suggests that, in the cases of incomplete or short hindcasts, the model may be more suitable to fill the gaps of missing intervals than to perform a resource assessment.

Following, the ANN model will be tested using a much comprehensive hindcast (23 years). Wave height from the site of that hindcast will be modeled using the proposed ANN model and a state-of-the-art nearshore model. Both models will be validated in that site with the aim to compare their performances.

3.2. Comparison of performances of the developed ANN model vs the Nearshore Wave Prediction System

Statistical comparisons between ocean wave models have been carried out frequently, for example SWAN vs. Wavewatch III [66]. In this section it is presented a direct comparison of results using the ANN model and the Nearshore Wave Prediction System (NWPS), which is a combination of several models: (SWAN, Wavewatch III and other simulators). The parameter that is compared is the significant wave height. That parameter is measured and registered every hour in a buoy station located in the West Coast of USA. There is a 23 years' significant wave height dataset from that buoy. The ANN model can be applied to that site by using that dataset as inputs, and then validated. In addition, the NWPS model is applied and validated in that site by the National Oceanic and Atmospheric Administration (NOAA), which turns possible a direct comparison between the performances of both models.

3.2.1. Origin of the data used for the comparison

NOAA is recognized worldwide for producing highly reliable ocean data and for making that data available online for the scientific community. It has several buoys deployed on the coasts of the USA that gather and transmit data. Among them, a buoy identified as Station 41004 was chosen for three main reasons. First,

it has a very similar water depth (38.4 m) than the other station located in the Brazilian coast. Secondly, it has an extent hindcast of wave height and period data with a frequency of 1 measurement per hour during 1994–2017. That allows developing and training an ANN model using a 23 years hindcast, which in thesis should produce a more accurate model than the one previously applied to the Brazilian coast (which only used data from the last 2½ years). Thirdly, the output of the NWPS model is validated using data from each buoy of the system, and the results of the validation for buoy 41004 were available for June 2017. This allows the comparison, for that site, of the NWPS model's performance against the ANN model. Fig. 8 shows buoy 41004 and its location in the West Coast of the USA.

Station 41004 is located 41 NM Southeast of Charleston, SC at 32°30′2" N 79°5′58" W. This 3-m foam buoy is owned and maintained by the National Data Buoy Center (NDBC). Besides counting with an extensive hindcast, this station also highlights for its sophisticated technology. It uses the state-of-the-art of NDBC's ocean observing system for buoys, named the Self-Contained Ocean Observing Payload (SCOOP) [67]. Wave observation is performed through the Digital Directional Wave Module (DDWM). This module consists of a nine axis motion sensor and processor. The nine axis motion sensor consists in a combination of a 3-axis gyroscope, a 3-axis accelerometer and a 3-axis magnetometer. Resolution of the sensors are 0.1 m (for wave height) and 1.0s (for wave period), which gives a system accuracy of ±0.2 m (for wave height) and ±1.0s (for wave period) [68]. The error for the estimate of the significant wave height is RMS<0.10 m with a Mean Diff<0.01 m. The error for the average period is RMS<0.14s [67].

3.2.2. The ANN model particularized for this comparison

A neural network model similar as the one explained in the Methodology chapter (non-linear autoregressive exogenous model trained using backpropagation) was particularized for the hindcast of the buoy 41004. The ANN model parameters were recalculated. For this particular hindcast, the optimal number of neurons is 10. Performance (mse) is 0.0456 and MAPE is 5.27%; Regarding the error distribution, the mean value of the error is 0.86 and the standard deviation (sigma) is 7.87.

3.2.3. The NWPS model

NWPS is driven by forecaster-developed wind grids produced in AWIPS – Advanced Weather Interactive Processing System, which integrates meteorological, hydrological, satellite and radar data. It is also driven by wave boundary conditions from the operational Wavewatch III model. The nearshore wave model used is SWAN, a third-generation wave model developed at Delft University of Technology that uses as inputs wind, bottom and current conditions. Wave-current interaction is included using surface currents from the Real-Time Ocean Forecast System (RTOFS-Global). Tides and storm surge are accounted for using the Extratropical Surge and Tide Operational Forecast System (ESTOFS, extratropical conditions), or the probabilistic model P-SURGE (tropical conditions). NWPS uses computational grids that have a nearshore resolution of 1.8 km–500 m and produces fields of integral wave parameters, wave spectra, and individually tracked wave systems (Gerling-Hanson plots). Experimental rip current and total water level guidance is produced at 5 pilot WFOs [69-74].

3.2.4. Validation of both models using data from NDBC's station 41004

For each day of June 2017, both models generated a predicted wave height at the site for the following 24, 48, 72 and 96 h. Then the predicted values were validated with the observed (measured) values in the buoy's sensors. Results of the validation, for each one of the four forecasts (24 h, 48 h, 72 h and 96 h) are presented in a scatter plot with two axis: the height output of the model (Hs,mod) and the one observed in the buoy (Hs,obs). Each plot has 30 validation points, representing the days of June 2017. Scatter plots that compare observed VS modeled wave heights are widely used. For instance, such plots are available for the global Wavewatch III model for deep waters, which is validated using the observations from the Jason 2 satellite [75]. NOAA also uses scatter plots to validate the NWPS model and kindly provided the necessary data for this validation [76]. Figs. 9 and 10 show the validation of both models' forecasts at Station 41004.

The validation of the NPWS is expressed using two statistical parameters: the relative bias and the scatter index (SI) [76]. The bias refers to the mean error, or the difference between the estimated value (the output of the model) and the value observed in the buoy's sensors. The relative bias is the bias divided by the value observed in the buoy. The scatter index refers to the RMSE (root-mean square error) normalized by the mean value of the measurements. Therefore both parameters were calculated for each validation, and compared in Table 3.

As can be seen on Table 3, the ANN model presented a smaller relative bias in the estimates of all the four forecasts. The ANN model performed better in terms of relative bias. Meanwhile, predictions using NWPS showed less deviation. The ANN model had a significantly higher scatter index, particularly in long-range

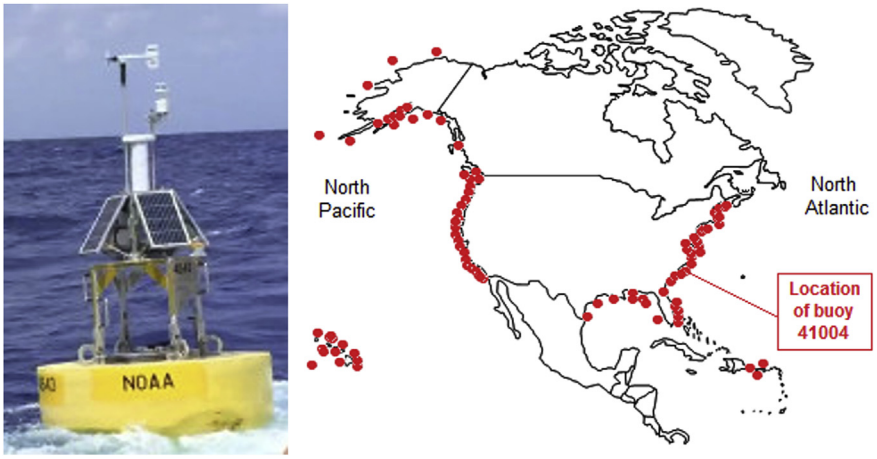

Fig. 8. Buoy 41004 and NOAA's system of data buoys.

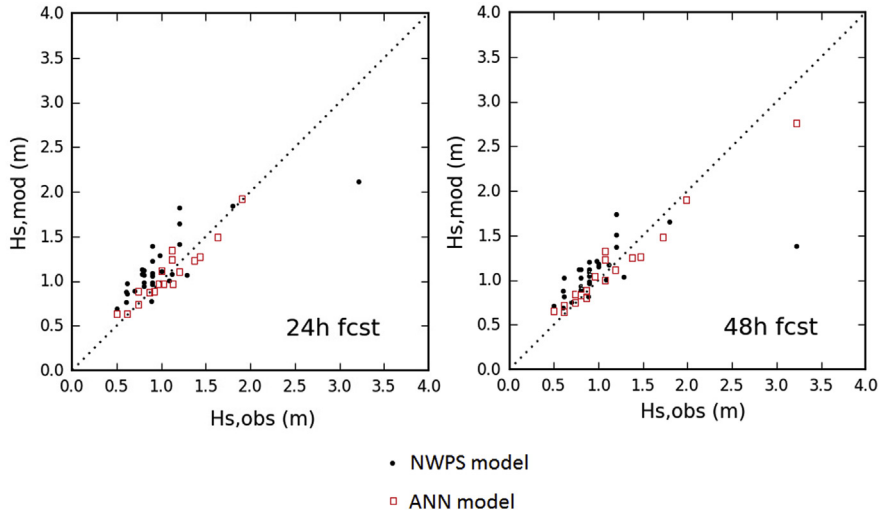

Fig. 9. Validation of ANN and NWPS models with data from Buoy 41004: Modeled VS Observed wave height, for 24 h and 48 h forecasts.

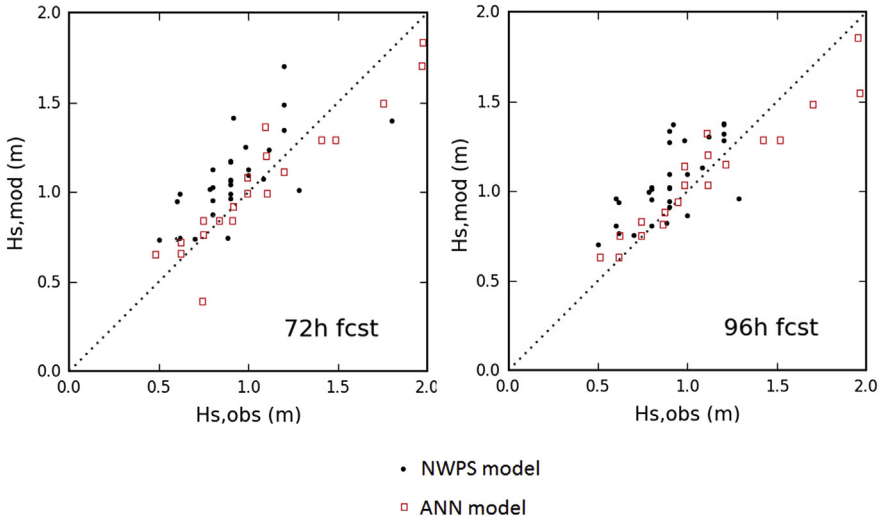

Fig. 10. Validation of ANN and NWPS models with data from Buoy 41004: Modeled VS Observed wave height, for 72 h and 96 h forecasts.

Table 3
Comparison between the performance of ANN and NWPS models for Buoy 41004 hindcast.

Relative bias and scatter index for each forecast		ANN model	NWPS
24 h	Rel. bias	0.0067	0.1560
	S.I.	0.4254	0.3320
48 h	Rel. bias	0.0130	0.0970
	S.I.	0.5154	0.4050
72 h	Rel. bias	0.0158	0.1700
	S.I.	0.6200	0.2670
96 h	Rel. bias	0.0204	0.1690
	S.I.	0.7400	0.2460

forecasts of 72 and 96 h in advance.

Moreover, the ANN model performed much better when using a much comprehensive hindcast. The error of the model, measured by the MAPE and the standard deviation, reduces when considering a more extent hindcast. The error of the model was too high for a 2½ years' dataset, which suggests a better use for filling the missing gaps than for resource assessment. Where there is enough data available (long-term datasets as recommended by international protocols) the ANN model could also have a use for resource assessment. By using a 23 years' hindcast, the ANN model was able to estimate the waves' height at Station 41004 with a MAPE of 5.27%. Table 4 shows a comparison between the performances of the proposed ANN model for the two hindcasts that were considered.

Table 4
Performance of the proposed ANN model with regards of the hindcast's extension.

	Bahia, Brazilian Coast	SC, West Coast of USA
Extension of the hindcast	Nov 2014 - May 2017 (2½ years)	Jan 1994 - June 2017 (23½ years)
Instrumentation used for wave data acquisition	acoustic doppler current profiler	nine axis motion sensor
Type of forecasting model	ANN (non-linear autoregressive exogenous model trained using backpropagation)	
MAPE	7.20%	5.27%
MSE	7.0200	0.0456
Mean value of the error distribution (μ)	7.20	0.86
Standard deviation of the error distribution (σ)	29.60	7.87
Coefficient of Variation (CV)	411%	915%

4. Conclusions

Wave monitoring systems have greatly evolved in recent years. Nautical radars, ADCPs, lidars, displacement and GPS buoys and stereo vision instrumentation are now available to produce high resolution data. Those data, in particular measures of wave height and period, are of interest for the assessment of the wave energy potential of coastal sites.

This research proposes a mathematical model, based on artificial neural networks, that uses direct wave measures to characterize that potential. The model selects some data from a hindcast and uses those values to train a neural network that estimates wave height and period, and therefore the wave power available in that particular coastal site. The model was implemented and validated in two different sites. The first one had a dataset from an acoustic Doppler wave profiler deployed at 32 m depth, measuring during 2½ years at intervals of 3 h. The second consisted in data from a buoy that deployed a 9-axis motion sensor and other instruments, and measured continuously during 23 years at intervals of 1 h.

In the first case (2½ years' hindcast) it was able to estimate the energy potential of the site with a mean error of 7.2%. By using a 23 years' hindcast, the mean error of the model decreased to 5.27% with much less deviation. The performance (precision and accuracy) of the ANN that is proposed in this research increases with the use of hindcasts covering longer periods. Moreover, when compared with the nearshore numerical model NPWS, the neural network trained with the 23 years' dataset performed quite well (better in terms of relative bias and worse in terms of scatter index). For datasets covering short periods of time, as in the first case, the error of the model is too high which suggests a better use for filling the missing gaps than for resource assessment. That is, given an incomplete set of measures from a coastal site, the remaining behavior of the waves in the missing gaps can be easily inferred with the use of this proposed model at an acceptable error. In sum, ANNs and other artificial intelligence algorithms are powerful computational tools that can make an optimal use of the data produced by wave monitoring instrumentation.

Acknowledgements

The authors sincerely thank the Brazilian Navy, GOOS Brazil and all the people involved in the Rede Ondas project, for making the data available and for its support during this research. We also thank NOAA for making their data available online. This work was supported by the Federal University of Bahia and by CAPES, the Brazilian Federal Agency for Post-graduate Education.

References

[1] S. Astariz, G. Iglesias, The economics of wave energy: a review, Renew. Sust. Energ Rev. 45 (2015) 397–408, http://dx.doi.org/10.1016/j.rser.2015.01.061.
[2] L. Rusu, C.G. Soares, Wave energy assessments in the Azores islands, Renew. Energy 45 (2012) 183–196, http://dx.doi.org/10.1016/j.renene.2012.02.027.
[3] F. Flocard, D. Ierodiaconou, I.R. Coghlan, Multi-criteria evaluation of wave energy projects on the south-east Australian coast, Renew. Energy 99 (2016) 80–94, http://dx.doi.org/10.1016/j.renene.2016.06.036.
[4] S.A. Sannasiraj, V. Sundar, Assessment of wave energy potential and its harvesting approach along the Indian coast, Renew. Energy 99 (2016) 398–409, http://dx.doi.org/10.1016/j.renene.2016.07.017.
[5] S. Wu, C. Liu, X. Chen, Offshore wave energy resource assessment in the East China Sea, Renew. Energy 76 (2015) 628–636, http://dx.doi.org/10.1016/j.renene.2014.11.054.
[6] S.C. Parkinson, K. Dragoon, G. Reikard, G. García-Medina, H.T. Özkan-Haller, T.K.A. Brekken, Integrating ocean wave energy at large-scales: a study of the US Pacific Northwest, Renew. Energy 76 (2015) 551–559, http://dx.doi.org/10.1016/j.renene.2014.11.038.
[7] E.B.L. Mackay, A.S. Bahaj, P.G. Challenor, Uncertainty in wave energy resource assessment. Part 1: historic data, Renew. Energy 35 (2010a) 1792–1808, http://dx.doi.org/10.1016/j.renene.2009.10.026.
[8] E.B.L. Mackay, A.S. Bahaj, P.G. Challenor, Uncertainty in wave energy resource assessment. Part 2: variability and predictability, Renew. Energy 35 (2010b) 1809–1819, http://dx.doi.org/10.1016/j.renene.2009.10.027.
[9] P. Pinson, G. Reikard, J. Bidlot, Probabilistic forecasting of the wave energy flux, Appl. Energy (2011), http://dx.doi.org/10.1016/j.apenergy.2011.12.040.
[10] G. Reikard, B. Robertson, B. Buckham, J.-R. Bidlot, C. Hiles, Simulating and forecasting ocean wave energy in western Canada, Ocean. Eng. 103 (2015) 223–236, http://dx.doi.org/10.1016/j.oceaneng.2015.04.081.
[11] D. Ingram, G.H. Smith, C. Ferriera, H. Smith, Protocols for the Equitable Assessment of Marine Energy Converters, The Institute for Energy Systems, Edinburgh, on behalf of the EquiMar project consortium, 2011.
[12] H. Smith, Best Practice Guidelines for Wave and Current Resource Assessment - Task 1.6 of WP3, Report from the MERiFIC Project - Marine Energy in Far Peripheral and Island Communities. MERiFIC Project, University of Exeter and Ifremer, 2014.
[13] H. Smith, C. Maisondieu, Resource Assessment for Cornwall, Isles of Scilly and PNMI - Task 1.2 of WP3, Report from the MERiFIC Project - Marine Energy in Far Peripheral and Island Communities. MERiFIC Project, University of Exeter and Ifremer, 2014.
[14] S.N. Londhe, S. Shah, P.R. Dixit, T.M.B. Nair, P. Sirisha, R. Jain, A coupled numerical and artificial neural network model for improving location specific wave forecast, Appl. Ocean. Res. 59 (2016) 483–491, http://dx.doi.org/10.1016/j.apor.2016.07.004.
[15] P. Dixit, S. Londhe, Y. Dandawate, Removing prediction lag in wave height forecasting using Neuro - wavelet modeling technique, Ocean. Eng. 93 (2015) 74–83, http://dx.doi.org/10.1016/j.oceaneng.2014.10.009.
[16] M. Özger, Significant wave height forecasting using wavelet fuzzy logic approach, Ocean. Eng. 37 (16) (2010) 1443–1451, http://dx.doi.org/10.1016/j.oceaneng.2010.07.009.
[17] P. Jain, M.C. Deo, Real-time wave forecasts off the western Indian coast, Appl. Ocean. Res. 29 (1–2) (2007) 72–79, http://dx.doi.org/10.1016/j.apor.2007.05.003.
[18] S. Mandal, N. Prabaharan, Ocean wave forecasting using recurrent neural networks, Ocean. Eng. 33 (10) (2006) 1401–1410, http://dx.doi.org/10.1016/j.oceaneng.2005.08.007.
[19] S.N. Londhe, V. Panchang, One-day wave forecasts based on artificial neural networks, J. Atmos. Ocean. Tech. 23 (11) (2006) 1593–1603, http://dx.doi.org/10.1175/JTECH1932.1.
[20] O. Makarynskyy, Neural pattern recognition and prediction for wind wave data assimilation, Pac. Oceanogr. 3 (2) (2006) 76–85.
[21] O. Makarynskyy, A.A. Pires-Silva, D. Makarynska, C. Ventura-Soares, Artificial neural networks in wave predictions at the west coast of Portugal, Comput Geosci. 31 (4) (2005) 415–424, http://dx.doi.org/10.1016/j.cageo.2004.10.005.
[22] O. Makarynskyy, D. Makarynska, Wave prediction and data supplementation with artificial neural networks, J. Coast. Res. 23 (4) (2007) 951–960, http://dx.doi.org/10.2112/04-0407.1.
[23] O. Makarynskyy, D. Makarynska, E. Rusu, A. Gavrilov, Filling gaps in wave records with artificial neural networks, in: C. Guedes Soares, Y. Garbatov, N. Fonseca (Eds.), Maritime Transportation and Exploitation of Ocean and Coastal Resources, Taylor & Francis Group, London, 2005, pp. 1085–1091.
[24] Z. Zhang, C.W. Li, Y.S. Li, Y. Qi, Incorporation of artificial neural networks and

data assimilation techniques into a third-generation wind–wave model for wave forecasting, J. Hydroinform. 8 (1) (2006) 65–76, http://dx.doi.org/10.2166/jh.2006.005.
[25] S. Mandal, S. Rao, D.H. Raju, Ocean wave parameters estimation using back-propagation neural networks, Mar. Struct. 18 (3) (2005) 301–318, http://dx.doi.org/10.1016/j.marstruc.2005.09.002.
[26] M.C. Deo, A. Jha, A.S. Chaphekar, K. Ravikant, Neural networks for wave forecasting, Ocean. Eng. 28 (7) (2001) 889–898, http://dx.doi.org/10.1016/S0029-8018(00)00027-5.
[27] M.C. Deo, C.S. Naidu, Real time wave forecasting using neural networks, Ocean. Eng. 26 (3) (1998) 191–203, http://dx.doi.org/10.1016/S0029-8018(97)10025-7.
[28] M.C. Deo, V. Venkat Rao, A. Sakar, Neural networks for wave height interpolation, Comput Aided Civ. Inf. 12 (1997) 217–225, http://dx.doi.org/10.1111/0885-9507.00058.
[29] O. Makarynskyy, Improving wave predictions with artificial neural networks, Ocean. Eng. 31 (5–6) (2004) 709–724, http://dx.doi.org/10.1016/j.oceaneng.2003.05.003.
[30] C.P. Tsai, C. Lin, J.N. Shen, Neural network for wave forecasting among multi-stations, Ocean. Eng. 29 (13) (2002) 1683–1695, http://dx.doi.org/10.1016/S0029-8018(01)00112-3.
[31] C. Balas, L. Koç, L. Balas, Predictions of missing wave data by recurrent neuronets, J. Waterw. Port. Coast. Ocean. Eng. 130 (5) (2004) 256–265, http://dx.doi.org/10.1061/(ASCE)0733-950X(2004)130:5(256).
[32] J.D. Agrawal, M.C. Deo, On-line wave prediction, Mar. Struct. 15 (1) (2002) 57–74, http://dx.doi.org/10.1016/S0951-8339(01)00014-4.
[33] M.C. Deo, N.K. Kumar, Interpolation of wave heights, Ocean. Eng. 27 (9) (2000) 907–919, http://dx.doi.org/10.1016/S0029-8018(99)00023-2.
[34] S. Bourdier, K. Dampney, H. Fernandez, G. Lopez, J.B. Richon, Non-Intrusive Wave Field Measurement, MARINET - Marine Renewables Infrastructure Network, MARINET deliverable D4.05, Rev. 4, 2014.
[35] COST - European Cooperation in Science and Technology, Measuring and Analysing the Directional Spectra of Ocean Waves - Working Group 3, COST Action714, EU Publications Office, 2005.
[36] ACT - Alliance for Coastal Technologies, Waves Measurement Systems Test and Evaluation Protocols, University of Maryland Center of Environmental Science, USA, 2012.
[37] R. Birch, D. Fissel, K. Borg, V. Lee, D. English, The capabilities of doppler current profilers for directional wave measurements in coastal and nearshore waters, in: Oceans '04 MTS/IEEE, 2004. Kobe, Japan.
[38] D.A. Mayer, J.I. Virmani, R.H. Weisberg, Velocity comparisons from upward and downward acoustic doppler current profilers on the West Florida shelf, J. Atmos. Ocean. Tech. 24 (2007) 1950–1960, http://dx.doi.org/10.1175/JTECH2094.1.
[39] H.E. Seim, C.R. Edwards, Comparison of buoy-mounted and bottom-moored ADCP performance at Gray's reef, J. Atmos. Ocean. Tech. 24 (2007) 270–284, http://dx.doi.org/10.1175/JTECH1972.1.
[40] J.T. Carvalho, Simulação da distribuição de energia das ondas oceânicas ao largo do litoral brasileiro (Thesis), INPI – National Institute of Space Research, Brazil, 2010.
[41] E.R. Beserra, A.L.T. Mendes, S.F. Estefen, C.E. Parente, Wave climate analysis for a wave energy conversion application in Brazil, in: ASME 26th International Conference on Offshore Mechanics and Arctic Engineering, OMAE2007-29597, 2007, pp. 897–902, http://dx.doi.org/10.1115/OMAE2007-29597. San Diego, USA.
[42] L.E. Assis, Avaliação e aproveitamento da energia de ondas oceânicas no litoral do Rio Grande do Sul (Thesis), Federal University of Rio Grande do Sul, Porto Alegre, Brazil, 2010.
[43] Teledyne RD Instruments Inc., http://rdinstruments.com/product/adcp/sentinel-adcp, 2009 (Accessed 28 October 2016).
[44] H. Walden, K. Richter, W. Sell, D.J. Olbers, A. Meerburg, E. Bouws, K. Enke, Measurements of Wind-wave Growth and Swell Decay during the Joint North Sea Wave Project (JONSWAP), 1973, pp. 8–12. Ergänzungsheft.
[45] J. Pastor, Y. Liu, Wave energy resource analysis for use in wave energy conversion, J. Offshore Mech. Arct. Eng. 137 (2015) 0119031–0119039, http://dx.doi.org/10.1115/1.4028880.
[46] B. Cahill, T. Lewis, Wave period ratios and the calculation of wave power, Proceedings of the 2nd Marine Energy Technology Symposium - METS2014 (Vol. 10), April 15-18, 2014, Seattle, WA.
[47] S.M. Calisal, A note on the derivation of potential energy for two dimensional water waves, Ocean. Eng. 10 (2) (1983) 133–138, http://dx.doi.org/10.1016/0029-8018(83)90019-7.
[48] A. Al-Habaibeh, D. Su, J. McCague, A. Knight, An innovative approach for energy generation from waves, Energy Convers. Manag. 51 (8) (2010) 1664–1668, http://dx.doi.org/10.1016/j.enconman.2009.11.041.
[49] E. Pitt, Estimating Power from Wave Measurements at the European Marine Energy Center (EMEC) Test Site, AWR, 2005.
[50] J.J. Song, S. Park, Neural model predictive control for nonlinear chemical processes, J. Chem. Eng. Jpn. 26 (4) (1993) 347–354, http://dx.doi.org/10.1252/jcej.26.347.
[51] C. Wang, K.U. Klatt, G. Dünnebier, S. Engell, F. Hanisch, Neural network-based identification of SMB chromatographic processes, Control Eng. Pract. 11 (8) (2003) 949–959, http://dx.doi.org/10.1016/S0967-0661(02)00212-5.
[52] M.C.B. Costa, A.L. Jardini, M.R.W. Maciel, M. Embiruçu, R.M. Filho, Empirical models for end-use properties prediction of LDPE: application in the flexible plastic packaging industry, Mater Res. 11 (1) (2008) 23–30, http://dx.doi.org/10.1590/S1516-14392008000100005.
[53] R.A. Noor, Z. Ahmad, M. Don, M.H. Uzir, Modelling and control of different types of polymerization processes using neural networks technique: a review, Can. J. Chem. Eng. 88 (6) (2010) 1065–1084, http://dx.doi.org/10.1002/cjce.20364.
[54] S. Haykin, Neural Network: a Comprehensive Foundation, 2nd edition, Prentice Hall PTR Upper Saddle River, NJ, USA, 1999.
[55] J. Nazari, O.K. Ersoy, Implementation of back-propagation neural networks with MatLab, ECE Tech. Rep. 275 (1992). http://docs.lib.purdue.edu/ecetr/275.
[56] C.G. Piuleac, M.A. Rodrigo, P. Cañizares, S. Curteanu, C. Sáez, Ten steps modeling of electrolysis processes by using neural networks, Environ. Modell. Softw. 25 (1) (2010) 74–81, http://dx.doi.org/10.1016/j.envsoft.2009.07.012.
[57] F.S. Mjalli, A.S. Ibrehem, Optimal hybrid modeling approach for polymerization reactors using parameter estimation techniques, Chem. Eng. Res. Des. 89 (7) (2011) 1078–1087, http://dx.doi.org/10.1016/j.cherd.2010.11.018.
[58] I. Bessa, C. Quito, K. Pontes, Artificial Neural Networks Structure Selection: the benefits of Cross Validation Method, EngOpt 2014: 4th International Conference on Engineering Optimization. Lisbon, 8-11th Sep 2014.
[59] B. Schenker, M. Agarwal, Cross-validated structure selection for neural networks, Comput Chem. Eng. 20 (2) (1996) 175–186, http://dx.doi.org/10.1016/0098-1354(95)00013-R.
[60] G.J. Bowden, H.R. Maier, G.C. Dandy, Optimal division of data for neural network models in water resources applications, Water Resour. Res. 38 (2) (2002) 2–11, http://dx.doi.org/10.1029/2001WR000266.
[61] S. Hoque, B. Farouk, C.N. Haas, Development of metamodels for predicting aerosol dispersion in ventilated spaces, Atmos. Environ. 45 (10) (2011) 1876–1887, http://dx.doi.org/10.1016/j.atmosenv.2010.12.046.
[62] G. Lavidas, V. Venugopal, D. Friedrich, Wave energy extraction in Scotland through an improved nearshore wave atlas, Int. J. Mar. Energy 17 (2017) 64–83, http://dx.doi.org/10.1016/j.ijome.2017.01.008.
[63] V. Venugopal, R. Nemalidinne, Wave resource assessment for Scottish waters using a large scale North Atlantic spectral wave model, Renew. Energy 76 (2015) 503–525, http://dx.doi.org/10.1016/j.renene.2014.11.056.
[64] B.G. Reguero, M. Menéndez, F.J. Méndez, R. Mínguez, I.J. Losada, A Global Ocean Wave (GOW) calibrated reanalysis from 1948 onwards, Coast. Eng. 65 (2012) 38–55, http://dx.doi.org/10.1016/j.coastaleng.2012.03.003.
[65] J. Perez, M. Menéndez, I.J. Losada, GOW2: a global wave hindcast for coastal applications, Coast. Eng. 124 (2017) 1–11, http://dx.doi.org/10.1016/j.coastaleng.2017.03.005.
[66] R.D. Montoya, A.O. Arias, J.C.O. Royero, F.J. Ocampo-Torres, A wave parameters and directional spectrum analysis for extreme winds, Ocean. Eng. 67 (2013) 100–118, http://dx.doi.org/10.1016/j.oceaneng.2013.04.016.
[67] P.E.C. Kohler, L. LeBlanc, J. Elliott, SCOOP - NDBC's New Ocean Observing System, OCEANS 2015-MTS/IEEE Washington, 2015, pp. 1–5, http://dx.doi.org/10.23919/OCEANS.2015.7401834. Washington, DC.
[68] R.E. Riley, National Data Buoy Center Wave System Refresh, NOAA's National Data Buoy Center,, Stennis Space Center, MS, USA, 2016. Available at: https://nosc.noaa.gov/2016_NOAA_ETW/5_Posters/Oceans_Riley_NDBC%20Wave%20System_FINAL_Revision%20(1).pdf.
[69] A. Gibbs, G. Dusek, A.J. van der Westhuysen, P. Santos, S. Stripling, S. Huddleston, E. Rivera-Acevedo, J. Estupinan, H. Seim, Numerical validation of a coupled probabilistic rip current model and Nearshore Wave Prediction System for South Florida, in: Proc. 95th AMS Annual Meeting, Am. Meteor. Soc., Phoenix, 2015.
[70] G. Dusek, A.J. van der Westhuysen, A. Gibbs, D. King, S. Kennedy, R. Padilla, H. Seim, D. Elder, Coupling a rip current forecast model to the nearshore wave prediction system, in: Proc. 94th AMS Annual Meeting, Am. Meteor. Soc., Atlanta, 2014.
[71] A.J. van der Westhuysen, A.A. Taylor, R. Padilla-Hernandez, A. Gibbs, P. Santos, D. Gaer, H.D. Cobb III, J.R. Lewitsky, J.R. Rhome, Enhancements to the Nearshore Wave Prediction System to provide coastal and overland hurricane wave guidance, in: Proc. 94th AMS Annual Meeting, Am. Meteor. Soc., Atlanta, 2014.
[72] A.J. van der Westhuysen, R. Padilla-Hernandez, P. Santos, A. Gibbs, D. Gaer, T. Nicolini, S. Tjaden, E.M. Devaliere, H.L. Tolman, Development and validation of the nearshore wave prediction system, in: Proc. 93rd AMS Annual Meeting, Am. Meteor. Soc., Austin, 2013.
[73] A.P. Gibbs, A.J. Santos, J. van der Westhuysen, R. Padilla-Hernandez, NWS Southern Region numerical optimization and sensitivity evaluation in non-stationary SWAN Simulations, in: Proc. 92nd AMS Annual Meeting, Am. Meteor. Soc., New Orleans, 2012.
[74] J.B. Settelmaier, A. Gibbs, P. Santos, T. Freeman, D. Gaer, Simulating waves nearshore (SWAN) modeling efforts at the national weather service (NWS) southern region (SR) coastal weather forecast offices (WFOs), in: Proc. 91st AMS Annual Meeting, Am. Meteor. Soc., Seattle, 2011.
[75] CPTEC/INPE – Center for Weather Forecasting and Climatic Studies, Avaliacão do modelo de ondas, 2017. São Paulo, Brazil. Available at: http://ondas.cptec.inpe.br/~rondas/pdf/ex_avaliacao.pdf.
[76] NOAA's National Weather Service, National Oceanic and Atmospheric Administration (NOAA). Nearshore Wave Prediction System, July 2017. Available at: http://polar.ncep.noaa.gov/nwps/viewer.shtml.